



Data Analysis and Irregularity Measurements in the Identical Structures of Carbon Nanocones $CNC_t(m)$

Kamel Jebreen^{1,2,3,*}, Hassan Kanj⁴, Inad Nawajah⁵, Nancy Chendeb⁶, Rami M. Amro¹

¹ Faculty of Applied Sciences, Palestine Technical University - Kadoorie, Hebron, Palestine

² Department of Mathematics, An-Najah National University, Nablus, Palestine

³ Unité de Recherche Clinique Saint-Louis Fernand-Widal Lariboisière, APHP, Paris, France

⁴ College of Engineering and Technology, American University of the Middle East, Egaila 54200, Kuwait

⁵ Department of Mathematics, Hebron University, Hebron, Palestine

⁶ Department of Computer Science, DeVinci Engineering Shcool, La Défense, 92916 Paris, France , France

Abstract. Irregularity indices are topological indices by nature. They are highly helpful for determining the quantitative topography of nonregular graphs' molecular structures. Both the quantitative structure-property relationship (QSPR) and the quantitative structure-activity relationship (QSAR) depend heavily on the computation of abnormalities in a graph. It is made up of several chemical and physical characteristics, including resistance, enthalpy, entropy, toxicity, melting and boiling points, and entropy. This paper examines the application of different irregularity indices to identify irregularity measurements (IMs) in the network of carbon nanocone molecules $CNC_t(m)$, for $t = 4, 5$, and t . We have used different irregularity indices such as $Irdif(\xi_t)$, $Al(\xi_t)$, $Irl(\xi_t)$, $Irlu(\xi_t)$, $Irlf(\xi_t)$, $Irf(\xi_t)$, $Irla(\xi_t)$, $Ird1(\xi_t)$, $Ira(\xi_t)$, $Irga(\xi_t)$, $Irb(\xi_t)$ & $Irr_t(\xi_t)$. Comparative graphic measures of irregularity in $CNC_4(m)$, $CNC_5(m)$ and $CNC_t(m)$ have also been examined and presented. We are interested in creating new formulas to gain a better understanding of irregularity measures in carbon nanocones using the indices described above.

2020 Mathematics Subject Classifications: 05C09, 05C10, 05C12, 05C31, 05C07, 05C10, 05C90, 05C92

Key Words and Phrases: Carbon nanocones, graphical measurements, vertex degree, edges, irregularity

*Corresponding author.

DOI: <https://doi.org/10.29020/nybg.ejpam.v18i1.5599>

Email addresses: Kamel.Jebreen@ptuk.edu.ps (K. Jebreen),
hassan.kanj@caum.edu.kw (H. Kanj), nancy.chendeb@devinci.fr (N. Chendeb),
inadn@hebron.edu (I. Nawaja), r.amro@ptuk.edu.ps (R. Amro)

1. Introduction

The most significant and fascinating element in existence is carbon. Without carbon, life on Earth would not be conceivable. It makes up the majority of the body's fats, proteins, carbohydrates, muscular tissue, and DNA. It is a non-metallic molecular component that is produced cosmically when helium burns. Technology based on atoms and molecules is known as nanotechnology. It comprises the design and decision-making involved in creating nanodevices. The use of carbon nanoparticles in nanotechnology [3, 9, 28] is crucial.

Carbon nanocones are structures that are conical in shape. They were invented in 1968 [12, 30]. They are useful for capping thin carbon on ultrafine gold needles that are used in scanning probe microscopy [10, 15, 26]. Carbon nanostructures have various real-life applications, such as biosensors, energy storage, and gas sensors [2, 27]. Carbon nanocones are typically symbolized as $CNC_t(m)$. A topological descriptor (TD) is known as the irregularity index of a graph ξ_t if $(TD(\xi_t) \geq 0)$ and $TD(\xi_t) = 0$ iff ξ_t is a regular graph. Many researchers have described that the prediction and discrimination of irregularity indices are low [13, 25, 31]. The main motivation of this study is how irregularity indices give accurate results that are used in many fields like enthalpy and entropy. The irregularity indices [1, 14, 29, 33] are depicted in Table 1.

| Irregularity Indices | | |
|--|---|--|
| $Irr_s(\xi_t) = \frac{1}{2} \sum_{\rho\mu \in E(\xi_t)} d_\rho - d_\mu $ | $Ira(\xi_t) = \sum_{\rho\mu \in E(\xi_t)} \left(d_\rho^{-\frac{1}{2}} - d_\mu^{-\frac{1}{2}} \right)^2$ | $Irga(\xi_t) = \sum_{\rho\mu \in E(\xi_t)} \ln \frac{d_\rho + d_\mu}{2\sqrt{d_\rho \times d_\mu}}$ |
| $Al(\xi_t) = \sum_{\rho\mu \in E(\xi_t)} d_\rho - d_\mu $ | $Irdif(\xi_t) = \sum_{\rho\mu \in E(\xi_t)} \left \frac{d_\rho}{d_\mu} - \frac{d_\mu}{d_\rho} \right ^2$ | $Irla(\xi_t) = 2 \sum_{\rho\mu \in E(\xi_t)} \frac{ d_\rho - d_\mu }{d_\rho + d_\mu}$ |
| $Irf(\xi_t) = \sum_{\rho\mu \in E(\xi_t)} (d_\rho - d_\mu)^2$ | $Irlu(\xi_t) = \sum_{\rho\mu \in E(\xi_t)} \frac{ d_\rho - d_\mu }{\min(d_\rho, d_\mu)}$ | $Ird1(\xi_t) = \sum_{\rho\mu \in E(\xi_t)} \ln \{1 + d_\rho - d_\mu \}$ |
| $Irb(\xi_t) = \sum_{\rho\mu \in E(\xi_t)} \left(d_\rho^{\frac{1}{2}} - d_\mu^{\frac{1}{2}} \right)^2$ | $Irlf(\xi_t) = \sum_{\rho\mu \in E(\xi_t)} \frac{ d_\rho - d_\mu }{\sqrt{d_\rho \times d_\mu}}$ | $Irl(\xi_t) = \sum_{\rho\mu \in E(\xi_t)} \ln d_\rho - \ln d_\mu $ |

Table 1: Irregularity indices for $\xi_t = CNC_t(m)$, for $t = 4, 5$ and t .

2. Material and Methods

Let ξ_t be an undirected, connected, simple, and finite graph of Carbon nanocones where d_ρ and d_μ are the valencies of the nodes ρ and μ , respectively [18, 23]. It is symbolized as $CNC_t(m)$. We take the molecular structures of Carbon nanocones $CNC_t(m)$, for $t = 4, 5$ and t , and then different irregularity indices such as $Irdif(\xi_t)$, $Al(\xi_t)$, $Irl(\xi_t)$, $Irlu(\xi_t)$, $Irlf(\xi_t)$, $Irf(\xi_t)$, $Irla(\xi_t)$, $Ird1(\xi_t)$, $Ira(\xi_t)$, $Irga(\xi_t)$, $Irb(\xi_t)$ and $Irr_s(\xi_t)$ are computed. We have used the comparative study method of testing by choosing the different molecular structures of Carbon nanocones. We have applied twelve irregularity indices to four different Carbon nanocones that are $CNC_t(m)$, for $t = 4, 5$ and t . [4, 20].

3. Applications

The above-calculated irregularity descriptors for the chemical compound Carbon nanocones network symbolically represented by $\xi_t = CNC_t(m)$, for $t = 4, 5$ and t , can be used to

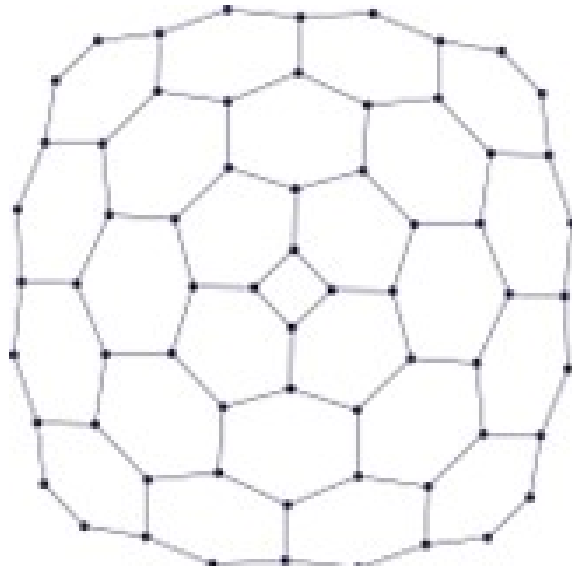
examine many physiochemical topographies [17, 19, 22]. Some of these topographies are given below:

- (i) Standard enthalpy of vaporization (DH_{VAP})
- (ii) Boiling point (B_P)
- (iii) Density
- (iv) Solubility.
- (v) Partition Coefficient.
- (vi) Ionization.
- (vii) Hydrogen Bonding.
- (viii) Chelation.
- (ix) Isosterism.
- (x) Entropy
- (xi) Surface activity.
- (xii) Enthalpy of vaporization (H_{VAP})
- (xiii) Melting point
- (xiv) Ionization energy.

Irregularity descriptors describe specific consequences about the above-mentioned chemical features [11, 16, 24]. Irregularity descriptors may support to explore also the chemical, biological, and nano properties that are extensively familiarized in developing parts of any country. Therefore, we calculate irregularity measurements for generalized version of $CNC_t(m)$, $t = 4, 5, \dots, n$ & $m = 1, 2, 3, \dots, n$.

4. Main Results and Discussion

We consider the molecular structures of Carbon nanocones $CNC_t(m)$, for $t = 4, 5$ and t shown in Figures 1-3. Let us choose $CNC_t(m)$ for $t = 4$ i.e., $CNC_4(m)$. We construct its molecular structure and apply different irregularity indices on it to get irregularity measurements. [6, 7, 21].

Figure 1: Graphical representation of CNC₄(m)

| d_μ | $ V(d_\mu) $ | (d_ρ, d_μ) | $ V(d_\rho, d_\mu) $ |
|---------|--------------|-------------------|----------------------|
| 2 | $4(m+1)$ | (2, 2) | 4 |
| 3 | $4m^2 + 4m$ | (2, 3) | $8m$ |
| - | - | (3, 3) | $2(3m^2 + m)$ |

Table 2: Depiction of the partition of edges of CNC₄(m).

With the help of Table 1 and Table 2, we have the following theorems:

Theorem 1 Let ξ_t be the molecular graph of Carbon nanocones CNC_t(m) with $t = 4$, then the irregularity indices are given by:

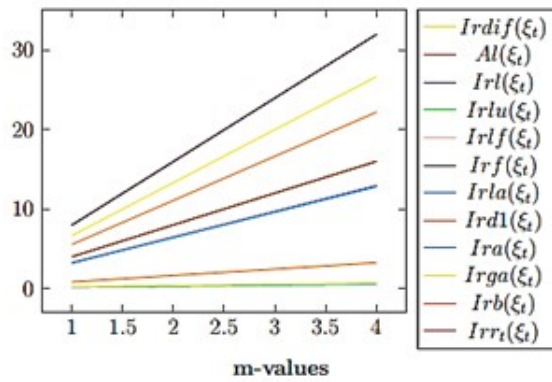
$$\begin{aligned}
\text{Irdif}(\xi_{t=4}) &= 50/9m \\
\text{Al}(\xi_{t=4}) &= 8m \\
\text{Irl}(\xi_{t=4}) &= 3.2437m \\
\text{Irlu}(\xi_{t=4}) &= 4m \\
\text{Irlf}(\xi_{t=4}) &= 3.2659m \\
\text{Irf}(\xi_{t=4}) &= 8m \\
\text{Irla}(\xi_{t=4}) &= 3.2m \\
\text{Ird 1}(\xi_{t=4}) &= 5.5451m \\
\text{Ira}(\xi_{t=4}) &= 0.1346m \\
\text{Irga}(\xi_{t=4}) &= 0.1632m \\
\text{Irb}(\xi_{t=4}) &= 0.8081m \\
\text{Ir } r_s(\xi_{t=4}) &= 4m
\end{aligned}$$

Proof. The cardinality of $\xi_{t=4}$ with respect to the vertices is $|V(\xi_{t=4})| = 4(m + 1)^2$ and the cardinality of $\xi_{t=4}$ with respect to the edges is $|E(\xi_{t=4})| = 2(3m^2 + 5m + 2)$. For this graph we identify (2, 2), (2, 3) and (3, 3) types of edges.

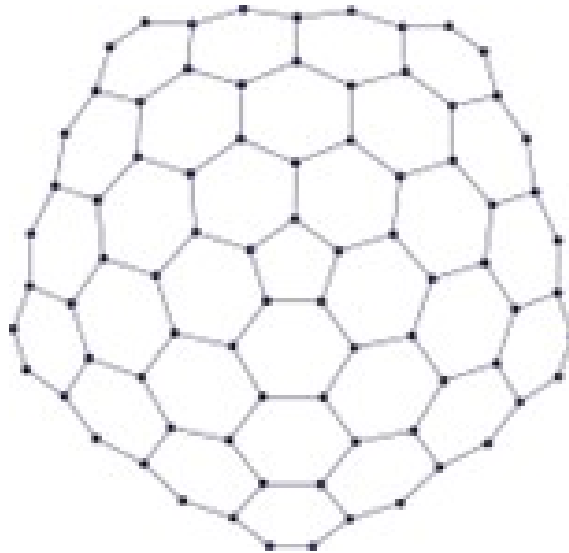
$$\begin{aligned}
\text{Irdif}(\xi_{t=4}) &= \sum_{\rho\mu \in E(\xi_{t=4})} \left| \frac{d_\rho}{d_\mu} - \frac{d_\mu}{d_\rho} \right| = \left(\sum_{\rho\mu \in E^{22}(\xi_{t=4})} + \sum_{\rho\mu \in E^{23}(\xi_{t=4})} + \sum_{\rho\mu \in E^{33}(\xi_{t=4})} \right) \left| \frac{d_\rho}{d_\mu} - \frac{d_\mu}{d_\rho} \right| = 6.67m. \\
\text{Al}(\xi_{t=4}) &= \sum_{\rho\mu \in E(\xi_{t=4})} |d_\rho - d_\mu| = \left(\sum_{\rho\mu \in E^{22}(\xi_{t=4})} + \sum_{\rho\mu \in E^{23}(\xi_{t=4})} + \sum_{\rho\mu \in E^{33}(\xi_{t=4})} \right) |d_\rho - d_\mu| = 8m. \\
\text{IrI}(\xi_{t=4}) &= \sum_{\rho\mu \in E(\xi_t)} |\ln d_\rho - \ln d_\mu| = \left(\sum_{\rho\mu \in E^{22}(\xi_{t=4})} + \sum_{\rho\mu \in E^{23}(\xi_{t=4})} + \sum_{\rho\mu \in E^{33}(\xi_{t=4})} \right) |\ln d_\rho - \ln d_\mu| = 3.243m. \\
\text{IrIlu}(\xi_{t=4}) &= \sum_{\rho\mu \in E(\xi_t)} \frac{|d_\rho - d_\mu|}{\min(d_\rho, d_\mu)} = \left(\sum_{\rho\mu \in E^{22}(\xi_{t=4})} + \sum_{\rho\mu \in E^{23}(\xi_{t=4})} + \sum_{\rho\mu \in E^{33}(\xi_{t=4})} \right) \frac{|d_\rho - d_\mu|}{\min(d_\rho, d_\mu)} = 4 \text{ m.} \\
\text{IrIlf}(\xi_{t=4}) &= \sum_{\rho\mu \in E(\xi_t)} \frac{|d_\rho - d_\mu|}{\sqrt{d_\rho \times d_\mu}} = \left(\sum_{\rho\mu \in E^{22}(\xi_{t=4})} + \sum_{\rho\mu \in E^{23}(\xi_{t=4})} + \sum_{\rho\mu \in E^{33}(\xi_{t=4})} \right) \frac{|d_\rho - d_\mu|}{\sqrt{d_\rho \times d_\mu}} = 3.2659 \text{ m.} \\
\text{IrIrf}(\xi_{t=4}) &= \sum_{\rho\mu \in E(\xi_t)} (d_\rho - d_\mu)^2 = \left(\sum_{\rho\mu \in E^{22}(\xi_{t=4})} + \sum_{\rho\mu \in E^{23}(\xi_{t=4})} + \sum_{\rho\mu \in E^{33}(\xi_{t=4})} \right) (d_\rho - d_\mu)^2 = 8m. \\
\text{IrIla}(\xi_{t=4}) &= 2 \sum_{\rho\mu \in E(\xi_t)} \frac{|d_\rho - d_\mu|}{d_\rho + d_\mu} = \left(\sum_{\rho\mu \in E^{22}(\xi_{t=4})} + \sum_{\rho\mu \in E^{23}(\xi_{t=4})} + \sum_{\rho\mu \in E^{33}(\xi_{t=4})} \right) \frac{|d_\rho - d_\mu|}{d_\rho + d_\mu} = 3.2m. \\
\text{IrId}(\xi_{t=4}) &= \sum_{\rho\mu \in E(\xi_t)} \ln \{1 + |d_\rho - d_\mu|\} = \left(\sum_{\rho\mu \in E^{22}(\xi_{t=4})} + \sum_{\rho\mu \in E^{23}(\xi_{t=4})} + \sum_{\rho\mu \in E^{33}(\xi_{t=4})} \right) \ln \{1 + |d_\rho - d_\mu|\} = 5.5451 \text{ m.} \\
\text{IrIa}(\xi_{t=4}) &= \sum_{\rho\mu \in E(\xi_t)} \left(d_\rho^{-\frac{1}{2}} - d_\mu^{-\frac{1}{2}} \right)^2 = \left(\sum_{\rho\mu \in E^{22}(\xi_{t=4})} + \sum_{\rho\mu \in E^{23}(\xi_{t=4})} + \sum_{\rho\mu \in E^{33}(\xi_{t=4})} \right) \left(d_\rho^{-\frac{1}{2}} - d_\mu^{-\frac{1}{2}} \right)^2 = 0.1346m. \\
\text{IrIga}(\xi_{t=4}) &= \sum_{\rho\mu \in E(\xi_t)} \ln \frac{d_\rho + d_\mu}{2\sqrt{d_\rho \times d_\mu}} = \left(\sum_{\rho\mu \in E^{22}(\xi_{t=4})} + \sum_{\rho\mu \in E^{23}(\xi_{t=4})} + \sum_{\rho\mu \in E^{33}(\xi_{t=4})} \right) \ln \frac{d_\rho + d_\mu}{2\sqrt{d_\rho \times d_\mu}} = 0.1632 \text{ m.} \\
\text{IrIrb}(\xi_{t=4}) &= \sum_{\rho\mu \in E(\xi_t)} \left(d_\rho^{\frac{1}{2}} - d_\mu^{\frac{1}{2}} \right)^2 = \left(\sum_{\rho\mu \in E^{22}(\xi_{t=4})} + \sum_{\rho\mu \in E^{23}(\xi_{t=4})} + \sum_{\rho\mu \in E^{33}(\xi_{t=4})} \right) \left(d_\rho^{\frac{1}{2}} - d_\mu^{\frac{1}{2}} \right)^2 = 0.8081 \text{ m.} \\
\text{IrIrs}(\xi_{t=4}) &= \frac{1}{2} \sum_{\rho\mu \in E(\xi_t)} |d_\rho - d_\mu| = \left(\sum_{\rho\mu \in E^{22}(\xi_{t=4})} + \sum_{\rho\mu \in E^{23}(\xi_{t=4})} + \sum_{\rho\mu \in E^{33}(\xi_{t=4})} \right) |d_\rho - d_\mu| = 4m.
\end{aligned}$$

All irregularity measurements for the Carbon nanocones network $CNC_4(m)$ by using the test values of parameter t , are shown in Table 3.

| Irregularity Indices | $m = 1$ | $m = 2$ | $m = 3$ | $m = 4$ |
|----------------------|---------|---------|---------|---------|
| $Irdif(\xi_t)$ | 5.58 | 11.12 | 16.68 | 22.24 |
| $Al(\xi_t)$ | 8 | 16 | 24 | 32 |
| $Irl(\xi_t)$ | 3.24 | 6.49 | 9.73 | 12.97 |
| $Irlu(\xi_t)$ | 4 | 8 | 12 | 16 |
| $Irlf(\xi_t)$ | 3.27 | 6.53 | 9.80 | 13.06 |
| $Irf(\xi_t)$ | 8 | 16 | 24 | 32 |
| $Irla(\xi_t)$ | 3.20 | 6.40 | 9.60 | 12.8 |
| $Ird1(\xi_t)$ | 5.55 | 11.10 | 16.65 | 22.2 |
| $Ira(\xi_t)$ | 0.13 | 0.27 | 0.40 | 0.54 |
| $Irga(\xi_t)$ | 0.16 | 0.33 | 0.49 | 0.65 |
| $Irb(\xi_t)$ | 0.81 | 1.62 | 2.42 | 3.23 |
| $Irr(\xi_t)$ | 4 | 8 | 12 | 16 |

Table 3: Depiction of irregularity indices with some test values for $\xi_4 = CNC_4(m)$.Graph I: Graphical Measurements of irregularity in $CNC_4(m)$.

Now, let us choose $CNC_t(m)$ for $t = 5$ i.e., $CNC_5(m)$. We construct its molecular structure and apply different irregularity indices to obtain irregularity measurements.

Figure 2: Molecular depiction of $CNC_5(m)$

| d_μ | $ V(d_\mu) $ | (d_ρ, d_μ) | $ V(d_\rho, d_\mu) $ |
|---------|--------------|-------------------|----------------------|
| 2 | $5(m+1)$ | (2, 2) | 5 |
| 3 | $5m^2 + 5m$ | (2, 3) | $10m$ |
| - | - | (3, 3) | $2.5(3m^2 + m)$ |

Table 4: Depiction of the partition of edges of $CNC_5(m)$.

With the help of Table 1 and Table 4, we have the following theorems.

Theorem 2. Let ξ_t be the molecular graph of Carbon nanocones $CNC_t(m)$ with $t = 5$, then the irregularity indices are given by:

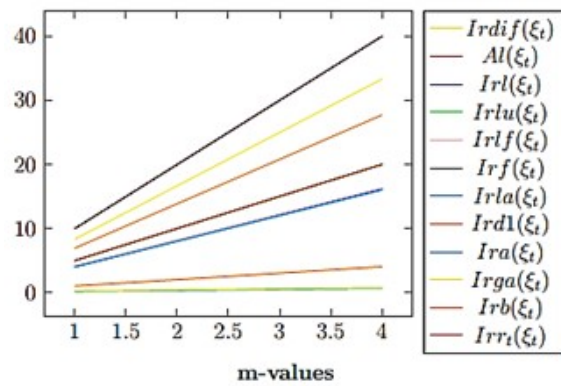
$$\begin{aligned}
 \text{Irdif}(\xi_{t=5}) &= 6.94 \text{ m} \\
 \text{Al}(\xi_{t=5}) &= 10 \text{ m} \\
 \text{Irl}(\xi_{t=5}) &= 4.0546 \text{ m} \\
 \text{Irlu}(\xi_{t=5}) &= 5 \text{ m} \\
 \text{Irlf}(\xi_{t=5}) &= 4.0824 \text{ m} \\
 \text{Irif}(\xi_{t=5}) &= 10 \text{ m} \\
 \text{Irla}(\xi_{t=5}) &= 4 \text{ m} \\
 \text{Ird1}(\xi_{t=5}) &= 6.9314 \text{ m} \\
 \text{Ira}(\xi_{t=5}) &= 0.1683 \text{ m} \\
 \text{Irga}(\xi_{t=5}) &= 0.2041 \text{ m} \\
 \text{Irb}(\xi_{t=5}) &= 1.0102 \text{ m} \\
 \text{Ir}_s(\xi_{t=5}) &= 5 \text{ m}.
 \end{aligned}$$

Proof. The cardinality of $\xi_{t=5}$ with respect to the vertices is $|V(\xi_{t=5})| = 5(m + 1)^2$ and the cardinality of $\xi_{t=5}$ with respect to the edges is $|E(\xi_{t=5})| = \frac{5}{2}(3m^2 + 5m + 2)$. We have found (2, 2), (2, 3) and (3, 3) types of edges.

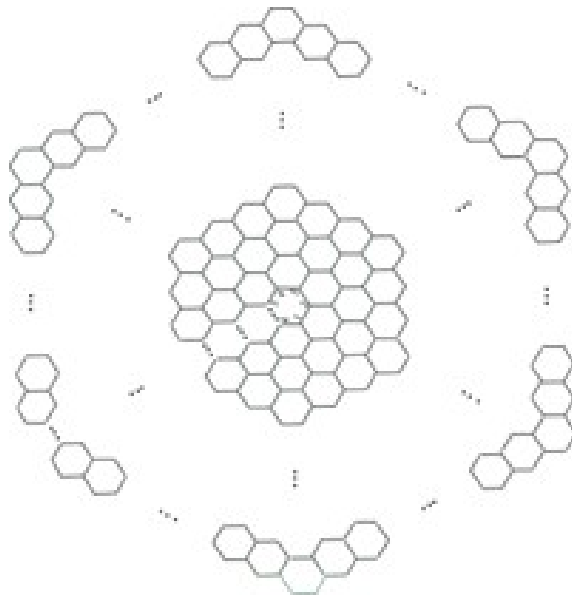
$$\begin{aligned}
\text{Irdif}(\xi_{t=5}) &= \sum_{\rho\mu \in E(\xi_{t=4})} \left| \frac{d_\rho}{d_\mu} - \frac{d_\mu}{d_\rho} \right| = \left(\sum_{\rho\mu \in E^{22}(\xi_{t=4})} + \sum_{\rho\mu \in E^{23}(\xi_{t=4})} + \sum_{\rho\mu \in E^{33}(\xi_{t=4})} \vdots ; \right) \left| \frac{d_\rho}{d_\mu} - \frac{d_\mu}{d_\rho} \right| = 8.33 \text{ m.} \\
\text{Al}(\xi_{t=5}) &= \sum_{\rho\mu \in E(\xi_{t=4})} |d_\rho - d_\mu| = \left(\sum_{\rho\mu \in E^{22}(\xi_{t=4})} + \sum_{\rho\mu \in E^{23}(\xi_{t=4})} + \sum_{\rho\mu \in E^{33}(\xi_{t=4})} \right) |d_\rho - d_\mu| = 10 \text{ m.} \\
\text{Irl}(\xi_{t=5}) &= \sum_{\rho\mu \in E(\xi_t)} |\ln d_\rho - \ln d_\mu| = \left(\sum_{\rho\mu \in E^{22}(\xi_{t=4})} + \sum_{\rho\mu \in E^{23}(\xi_{t=4})} + \sum_{\rho\mu \in E^{33}(\xi_{t=4})} \bar{i} \right) |\ln d_\rho - \ln d_\mu| = 4.0546 \text{ m.} \\
\text{Irlu}(\xi_{t=5}) &= \sum_{\rho\mu \in E(\xi_t)} \frac{|d_\rho - d_\mu|}{\min(d_\rho, d_\mu)} = \left(\sum_{\rho\mu \in E^{22}(\xi_{t=4})} + \sum_{\rho\mu \in E^{23}(\xi_{t=4})} + \sum_{\rho\mu \in E^{33}(\xi_{t=4})} \right) \frac{|d_\rho - d_\mu|}{\min(d_\rho, d_\mu)} = 5 \text{ m.} \\
\text{Irlf}(\xi_{t=5}) &= \sum_{\rho\mu \in E(\xi_t)} \frac{|d_\rho - d_\mu|}{\sqrt{d_\rho \times d_\mu}} = \left(\sum_{\rho\mu \in E^{22}(\xi_{t=4})} + \sum_{\rho\mu \in E^{23}(\xi_{t=4})} + \sum_{\rho\mu \in E^{33}(\xi_{t=4})} \right) \frac{|d_\rho - d_\mu|}{\sqrt{d_\rho \times d_\mu}} = 4.0824 \text{ m.} \\
\text{Irf}(\xi_{t=5}) &= \sum_{\rho\mu \in E(\xi_t)} (d_\rho - d_\mu)^2 = \left(\sum_{\rho\mu \in E^{22}(\xi_{t=4})} + \sum_{\rho\mu \in E^{23}(\xi_{t=4})} + \sum_{\rho\mu \in E^{33}(\xi_{t=4})} \right) (d_\rho - d_\mu)^2 = 10 \text{ m.} \\
\text{Irla}(\xi_{t=5}) &= 2 \sum_{\rho\mu \in E(\xi_t)} \frac{|d_\rho - d_\mu|}{d_\rho + d_\mu} = \left(\sum_{\rho\mu \in E^{22}(\xi_{t=4})} + \sum_{\rho\mu \in E^{23}(\xi_{t=4})} + \sum_{\rho\mu \in E^{33}(\xi_{t=4})} ; \frac{|d_\rho - d_\mu|}{d_\rho + d_\mu} \right) = 4 \text{ m.} \\
\text{Ird1}(\xi_{t=5}) &= \sum_{\rho\mu \in E(\xi_t)} \ln \{1 + |d_\rho - d_\mu|\} = \left(\sum_{\rho\mu \in E^{22}(\xi_{t=4})} + \sum_{\rho\mu \in E^{23}(\xi_{t=4})} + \sum_{\rho\mu \in E^{33}(\xi_{t=4})} ; \ln \{1 + |d_\rho - d_\mu|\} \right) \\
&= 6.9314 \text{ m.} \\
\text{Ira}(\xi_{t=5}) &= \sum_{\rho\mu \in E(\xi_t)} \left(d_\rho^{-\frac{1}{2}} - d_\mu^{-\frac{1}{2}} \right)^2 = \left(\sum_{\rho\mu \in E^{22}(\xi_{t=4})} + \sum_{\rho\mu \in E^{23}(\xi_{t=4})} + \sum_{\rho\mu \in E^{33}(\xi_{t=4})} \right) \left(d_\rho^{-\frac{1}{2}} - d_\mu^{-\frac{1}{2}} \right)^2 = 0.1683 \text{ m.} \\
\text{Irga}(\xi_{t=5}) &= \sum_{\rho\mu \in E(\xi_t)} \ln \frac{d_\rho + d_\mu}{2\sqrt{d_\rho \times d_\mu}} = \left(\sum_{\rho\mu \in E^{22}(\xi_{t=4})} + \sum_{\rho\mu \in E^{23}(\xi_{t=4})} + \sum_{\rho\mu \in E^{33}(\xi_{t=4})} ; \ln \frac{d_\rho + d_\mu}{2\sqrt{d_\rho \times d_\mu}} \right) = 0.2041 \text{ m.} \\
\text{Irb}(\xi_{t=5}) &= \sum_{\rho\mu \in E(\xi_t)} \left(d_\rho^{\frac{1}{2}} - d_\mu^{\frac{1}{2}} \right)^2 = \left(\sum_{\rho\mu \in E^{22}(\xi_{t=4})} + \sum_{\rho\mu \in E^{23}(\xi_{t=4})} + \sum_{\rho\mu \in E^{33}(\xi_{t=4})} \right) \left(d_\rho^{\frac{1}{2}} - d_\mu^{\frac{1}{2}} \right)^2 = 1.0102 \text{ m.} \\
\text{Irr}_s(\xi_{t=5}) &= \frac{1}{2} \sum_{\rho\mu \in E(\xi_t)} |d_\rho - d_\mu| = \left(\sum_{\rho\mu \in E^{22}(\xi_{t=4})} + \sum_{\rho\mu \in E^{23}(\xi_{t=4})} + \sum_{\rho\mu \in E^{33}(\xi_{t=4})} ; |d_\rho - d_\mu| \right) = 5 \text{ m.}
\end{aligned}$$

All irregularity measurements for the Carbon nanocones network CNC₅ (m) by using test values of parameter t , are shown in Table 5.

| Irregularity Indices | $m = 1$ | $m = 2$ | $m = 3$ | $m = 4$ |
|----------------------|---------|---------|---------|---------|
| $Irdif(\xi_t)$ | 6.94 | 13.88 | 20.80 | 27.76 |
| $Al(\xi_t)$ | 10 | 20 | 30 | 40 |
| $Irl(\xi_t)$ | 4.05 | 8.10 | 12.15 | 16.2 |
| $Irlu(\xi_t)$ | 5 | 10 | 15 | 20 |
| $Irlf(\xi_t)$ | 4.08 | 8.16 | 12.24 | 16.32 |
| $Irf(\xi_t)$ | 10 | 20 | 30 | 40 |
| $Irla(\xi_t)$ | 4 | 8 | 12 | 16 |
| $Ird1(\xi_t)$ | 6.93 | 13.86 | 20.79 | 27.72 |
| $Ira(\xi_t)$ | 0.17 | 0.34 | 0.51 | 0.68 |
| $Irga(\xi_t)$ | 0.20 | 0.40 | 0.60 | 0.80 |
| $Irb(\xi_t)$ | 1.01 | 2.02 | 3.03 | 4.04 |
| $Irr r_t(\xi_t)$ | 5 | 10 | 15 | 20 |

Table 5: Depiction of irregularity indices with some test values for $\xi_5 = CNC_5(m)$.Graph2: Graphical Measurements of irregularity in $CNC_5(m)$.

Now, let us choose $CNC_t(m)$ for $t = t$ i.e., $CNC_t(m)$. We construct its molecular structure and apply different irregularity indices to obtain irregularity measurements.

Figure 3: Graphical formation display of generalized form of $CNC_t(m)$

| d_μ | $ V(d_\mu) $ | (d_ρ, d_μ) | $ V(d_\rho, d_\mu) $ |
|---------|--------------|-------------------|----------------------|
| 2 | $t(m+1)$ | $(2, 2)$ | t |
| 3 | $t(m^2+m)$ | $(2, 3)$ | $2tm$ |
| - | - | $(3, 3)$ | $0.5t(3m^2+m)$ |

Table 6: Depiction of the partition of edges of $CNC_t(m)$.

With the help of Table 1 and Table 6, we have the following theorems.

Theorem 3. Let ξ_t be the molecular graph of Carbon nanocones $CNC_t(m)$ with $t = t$, then the irregularity indices are given by:

$$\text{Irdif}(\xi_t) = 1.3888\text{tm}$$

$$\text{Al}(\xi_t) = 2\text{tm}$$

$$\text{IrI}(\xi_t) = 0.8109\text{tm}$$

$$\text{Irlu}(\xi_t) = \text{tm}$$

$$\text{Irlf}(\xi_t) = 0.8164\text{tm}$$

$$\text{Irf}(\xi_t) = 2\text{tm}$$

$$\text{Irla}(\xi_t) = 0.4\text{tm}$$

$$\text{Ird1}(\xi_t) = 1.3862\text{tm}$$

$$\text{Ira}(\xi_t) = 0.0336\text{tm}$$

$$\text{Irga}(\xi_t) = 0.0408\text{tm}$$

$$\text{Irb}(\xi_t) = 0.2020\text{tm}$$

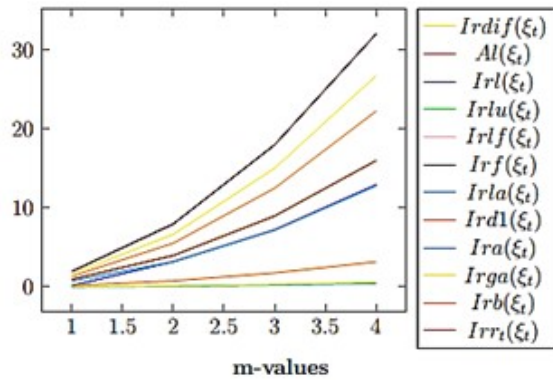
$$\text{Irr}(\xi_t) = \text{tm}$$

Proof. The cardinality of ξ_t with respect to the vertices is $|V(\xi_t)| = t(m + 1)^2$ and the cardinality of ξ_t with respect to the edges is $|E(\xi_t)| = \frac{t}{2}(3m^2 + 5m + 2)$. We have found $(2, 2)$, $(2, 3)$ and $(3, 3)$ types of edges.

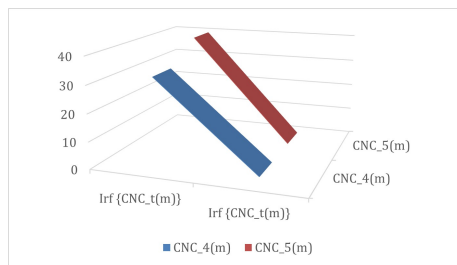
$$\begin{aligned}
\text{Irdif}(\xi_t) &= \sum_{\rho\mu \in E(\xi_{t=4})} \left| \frac{d_\rho}{d_\mu} - \frac{d_\mu}{d_\rho} \right| = \left(\sum_{\rho\mu \in E^{22}(\xi_{t=4})} + \sum_{\rho\mu \in E^{23}(\xi_{t=4})} + \sum_{\rho\mu \in E^{33}(\xi_{t=4})} \vdots \right) \left| \frac{d_\rho}{d_\mu} - \frac{d_\mu}{d_\rho} \right| = 1.6666\text{tm}. \\
\text{Al}(\xi_t) &= \sum_{\rho\mu \in E(\xi_{t=4})} |d_\rho - d_\mu| = \left(\sum_{\rho\mu \in E^{22}(\xi_{t=4})} + \sum_{\rho\mu \in E^{23}(\xi_{t=4})} + \sum_{\rho\mu \in E^{33}(\xi_{t=4})} \right) |d_\rho - d_\mu| = 2\text{tm}. \\
\text{Irl}(\xi_t) &= \sum_{\rho\mu \in E(\xi_t)} |\ln d_\rho - \ln d_\mu| = \left(\sum_{\rho\mu \in E^{22}(\xi_{t=4})} + \sum_{\rho\mu \in E^{23}(\xi_{t=4})} + \sum_{\rho\mu \in E^{33}(\xi_{t=4})} \vdots \right) |\ln d_\rho - \ln d_\mu| = 0.8109\text{tm}. \\
\text{Irлу}(\xi_t) &= \sum_{\rho\mu \in E(\xi_t)} \frac{|d_\rho - d_\mu|}{\min(d_\rho, d_\mu)} = \left(\sum_{\rho\mu \in E^{22}(\xi_{t=4})} + \sum_{\rho\mu \in E^{23}(\xi_{t=4})} + \sum_{\rho\mu \in E^{33}(\xi_{t=4})} ; \right) \frac{|d_\rho - d_\mu|}{\min(d_\rho, d_\mu)} = t\text{m}. \\
\text{Irlf}(\xi_t) &= \sum_{\rho\mu \in E(\xi_t)} \frac{|d_\rho - d_\mu|}{\sqrt{d_\rho \times d_\mu}} = \left(\sum_{\rho\mu \in E^{22}(\xi_{t=4})} + \sum_{\rho\mu \in E^{23}(\xi_{t=4})} + \sum_{\rho\mu \in E^{33}(\xi_{t=4})} \right) \frac{|d_\rho - d_\mu|}{\sqrt{d_\rho \times d_\mu}} = 0.8164\text{tm}. \\
\text{IrF}(\xi_t) &= \sum_{\rho\mu \in E(\xi_t)} (d_\rho - d_\mu)^2 = \left(\sum_{\rho\mu \in E^{22}(\xi_{t=4})} + \sum_{\rho\mu \in E^{23}(\xi_{t=4})} + \sum_{\rho\mu \in E^{33}(\xi_{t=4})} \right) (d_\rho - d_\mu)^2 = 2\text{tm}. \\
\text{Irla}(\xi_t) &= 2 \sum_{\rho\mu \in E(\xi_t)} \frac{|d_\rho - d_\mu|}{d_\rho + d_\mu} = \left(\sum_{\rho\mu \in E^{22}(\xi_{t=4})} + \sum_{\rho\mu \in E^{23}(\xi_{t=4})} + \sum_{\rho\mu \in E^{33}(\xi_{t=4})} \right) \frac{|d_\rho - d_\mu|}{d_\rho + d_\mu} = 0.8\text{tm}. \\
\text{Ird 1}(\xi_t) &= \sum_{\rho\mu \in E(\xi_t)} \ln \{1 + |d_\rho - d_\mu|\} = \left(\sum_{\rho\mu \in E^{22}(\xi_{t=4})} + \sum_{\rho\mu \in E^{23}(\xi_{t=4})} + \sum_{\rho\mu \in E^{33}(\xi_{t=4})} ; \ln \{1 + |d_\rho - d_\mu|\} \right) = 1.3862\text{tm}. \\
\text{Ira}(\xi_t) &= \sum_{\rho\mu \in E(\xi_t)} \left(d_\rho^{-\frac{1}{2}} - d_\mu^{-\frac{1}{2}} \right)^2 = \left(\sum_{\rho\mu \in E^{22}(\xi_{t=4})} + \sum_{\rho\mu \in E^{23}(\xi_{t=4})} + \sum_{\rho\mu \in E^{33}(\xi_{t=4})} \right) \left(d_\rho^{-\frac{1}{2}} - d_\mu^{-\frac{1}{2}} \right)^2 = 0.0336\text{tm}. \\
\text{Irga}(\xi_t) &= \sum_{\rho\mu \in E(\xi_t)} \ln \frac{d_\rho + d_\mu}{2\sqrt{d_\rho \times d_\mu}} = \left(\sum_{\rho\mu \in E^{22}(\xi_{t=4})} + \sum_{\rho\mu \in E^{23}(\xi_{t=4})} + \sum_{\rho\mu \in E^{33}(\xi_{t=4})} \right) \ln \frac{d_\rho + d_\mu}{2\sqrt{d_\rho \times d_\mu}} = 0.0408\text{tm}. \\
\text{IrB}(\xi_t) &= \sum_{\rho\mu \in E(\xi_t)} \left(d_\rho^{\frac{1}{2}} - d_\mu^{\frac{1}{2}} \right)^2 = \left(\sum_{\rho\mu \in E^{22}(\xi_{t=4})} + \sum_{\rho\mu \in E^{23}(\xi_{t=4})} + \sum_{\rho\mu \in E^{33}(\xi_{t=4})} \right) \left(d_\rho^{\frac{1}{2}} - d_\mu^{\frac{1}{2}} \right)^2 = 0.2020\text{tm}. \\
\text{Irr}_s(\xi_t) &= \frac{1}{2} \sum_{\rho\mu \in E(\xi_t)} |d_\rho - d_\mu| = \left(\sum_{\rho\mu \in E^{22}(\xi_{t=4})} + \sum_{\rho\mu \in E^{23}(\xi_{t=4})} + \sum_{\rho\mu \in E^{33}(\xi_{t=4})} \right) |d_\rho - d_\mu| = t\text{m}
\end{aligned}$$

All irregularity measurements for the Carbon nanocones network $CNC_t(m)$ by using test values of parameter m , are shown in Table 7 with their graphical representation in graph

| Irregularity Indices | $m = 1$ | $m = 2$ | $m = 3$ | $m = 4$ |
|----------------------|---------|---------|---------|---------|
| $Irdif(\xi_t)$ | 1.39 t | 2.78 t | 5.01 t | 5.56 t |
| $Al(\xi_t)$ | 2 t | 4 t | 6 t | 8 t |
| $Irl(\xi_t)$ | 0.81 t | 1.62 t | 2.43 t | 3.24 t |
| $Irlu(\xi_t)$ | t | 2 t | 3 t | 4 t |
| $Irlf(\xi_t)$ | 0.82 t | 1.64 t | 2.46 t | 3.28 t |
| $Irf(\xi_t)$ | 2 t | 4 t | 6 t | 8 t |
| $Irla(\xi_t)$ | 0.4 t | 0.8 t | 1.2 t | 1.6 t |
| $Ird1(\xi_t)$ | 1.39 t | 2.78 t | 4.17 t | 5.56 t |
| $Ira(\xi_t)$ | 0.03 t | 0.06 t | 0.09 t | 0.12 t |
| $Irga(\xi_t)$ | 0.04 t | 0.08 t | 0.12 t | 0.16 t |
| $Irb(\xi_t)$ | 0.20 t | 0.40 t | 0.60 t | 0.80 t |
| $Irrt(\xi_t)$ | t | 2 t | 3 t | 4 t |

Table 7: Depiction of irregularity indices with some test values for $\xi_t = CNC_t(m)$.Graph 3: Graphical Measurements of irregularity in $CNC_{t=1}(m)$.

| | $Irf(\xi_t)$ | $Ira(\xi_t)$ |
|------------|--------------|--------------|
| $CNC_4(m)$ | 32 | 0.54 |
| $CNC_5(m)$ | 40 | 0.68 |

Table 8: Shows the irregularity indices $Irf(\xi_t)$ and $Ira(\xi_t)$ for $\xi_t = CNC_{t=4,5}(m)$.Graph4: Graphical Analysis of irregularity in $CNC_{t=4,5}(m)$.

| IMs | $CNC_t(m)$, $t = 4, 5, \dots n \& m = 1, 2, 3, \dots n$ |
|-------------------|--|
| Irdif (ξ_t) | 1.39 tm |
| Al (ξ_t) | 2 tm |
| Irl (ξ_t) | 0.81 tm |
| Irlu (ξ_t) | tm |
| Irlf (ξ_t) | 0.82 tm |
| Irf (ξ_t) | 2 tm |
| Irla (ξ_t) | 0.40tm |
| Ird 1 (ξ_t) | 1.39 tm |
| Ira (ξ_t) | 0.03 tm |
| Irga (ξ_t) | 0.04tm |
| Irb (ξ_t) | 0.20 tm |
| Irr r_s) | tm |

Table 9: Shows the irregularity measurements with generalized form of Carbon nancones.

5. Conclusion

We analyse the theoretical and graphical data we acquired for the Carbon Nanocones network $CNC_t(m)$, for $t = 4, 5$ and t using the twelve irregularity indices described above. Based on these results, we determine which molecular network is more irregular than the others according to a certain irregularity index. It has been noted that, for $CNC_t(m)$, for $t = 4, 5$ and t , all of the generated graphs have a straight-line form, and all formulas derived from irregularity indices are linear in m and $CNC_t(m)$ are dependent on a parameter m . It has shown that increasing the parameter value causes the irregularity indices' value to grow as well. Graphs 1-2 show the graphic behaviour of IM for $CNC_t(m)$, for $t = 4, 5$.

The calculated and shown irregularity indices for $\xi_t = CNC_{t=4,5}(m)$ are presented in Table 8. The irregularity measurements for the generalized version of $CNC_t(m)$, $t = 4, 5, \dots n \& m = 1, 2, 3, \dots n$, are displayed in Table 9. The graphical behaviour of $CNC_4(m)$, $CNC_5(m)$ for the irregularity index $Ir f(\xi_t)$ is shown by the black line. On the other hand, graph 4 shows the graphical behavior of $CNC_4(m)$, $CNC_5(m)$ for the irregularity index $Ira(\xi_t)$, as represented by the pink line.

Moreover, a variety of physicochemical parameters, including those listed in Section 5 above, can be found and compared using irregularity indices [5, 8, 32]. Using irregularity indices, correlation, and the regression model $P = a + bX$, where X can be any topological index - we determine the experimental values of the fourteen physicochemical parameters listed above and then compare them to our estimated values. Additionally, we can contrast their major and non-significant errors. If we compute the fourteen physicochemical parameters listed above more accurately and numerically using irregularity indices, we do not require the experimental results.

It has also been observed that the difference of irregularity measurements for $Irf(\xi_t)$

among CNC_4 (m) and CNC_5 (m) are unified. Similarly, the difference of irregularity measurements for Ira (ξ_t) among CNC_4 (m) and CNC_5 (m) are same.

Acknowledgements

The authors extend their heartfelt gratitude to Palestine Technical University-Kadoorie, Palestine, American University of the Middle East, Egaila 54200, Kuwait, and ICTP-Arab Fund Associates Programme (2024-2026) for their invaluable support in facilitating this research.

Data Availability: All data used are included inside the manuscript.

References

- [1] Hosam Abdo, Stephan Brandt, and Darko Dimitrov. The total irregularity of a graph. *Discrete Mathematics & Theoretical Computer Science*, 16(Graph Theory), 2014.
- [2] Olumide O Adisa, Barry J Cox, and James M Hill. Modelling the surface adsorption of methane on carbon nanostructures. *Carbon*, 49(10):3212–3218, 2011.
- [3] Muhammad Haroon Aftab, Ali Akgül, Muhammad Bilal Riaz, Muhammad Athar Hussain, Kamel Jebreen, and Hassan Kanj. Measuring the energy for the molecular graphs of antiviral agents: Hydroxychloroquine, chloroquine and remdesivir. *South African Journal of Chemical Engineering*, 47(1):333–337, 2024.
- [4] Muhammad Haroon Aftab, Kamel Jebreen, Mohammad Issa Sowaity, and Muhammad Hussain. Analysis of eigenvalues for molecular structures. *Computers, Materials and Continua*, 73:1225–1236, 2022.
- [5] Muhammad Haroon Aftab, Kamel Jebreen, Mohammad Issa Sowaity, and Muhammad Hussain. Analysis of eigenvalues for molecular structures. *Computers, Materials and Continua*, 73:1225–1236, 2022.
- [6] Shams Al-duha Abu Alhassan, Abdulsader Nour, Sameh Atout, Zahran Daraghma, and Kamel Jebreen. Does corporate governance moderates the impact of earnings management on capital structure: Evidence from palestine and amman bourses. 2023.
- [7] Iftikhar Ali, Muhammad Haroon Aftab, Muhammad Waheed Raheed, Kamel Jebreen, Hassan Kanj, et al. Topological effects of chiral pamam dendrimer for the treatment of cancer. *Transylvanian Review*, 31(2), 2023.
- [8] Nawaf Ali, Tarek Khalifa, Hifza Iqbal, Muhammad Haroon Aftab, Kamel Jebreen, Humira Jamil, and Hassan Kanj. Graphical invariants for some transformed networks. *European Journal of Pure and Applied Mathematics*, 17(2):690–709, 2024.
- [9] Debnath Bhattacharyya, Shashank Singh, Niraj Satnalika, Ankesh Khandelwal, and Seung-Hwan Jeon. Nanotechnology, big things from a tiny world: a review. *International Journal of u-and e-Service, Science and Technology*, 2(3):29–38, 2009.
- [10] Abraham G Cano-Marquez, Wesller G Schmidt, Jenaina Ribeiro-Soares, Luiz Gustavo Cançado, Wagner N Rodrigues, Adelina P Santos, Clascidia A Furtado, Pedro AS Autreto, Ricardo Paupitz, Douglas S Galvão, et al. Enhanced mechanical stability of

- gold nanotips through carbon nanocone encapsulation. *Scientific Reports*, 5(1):10408, 2015.
- [11] Matthieu Falque, Kamel Jebreen, Etienne Paux, Carsten Knaak, Sofiane Mezmouk, and Olivier C Martin. Cnvmap: a method and software to detect and map copy number variants from segregation data. *Genetics*, 214(3):561–576, 2020.
 - [12] J Gillot, W Bollmann, and B Lux. Cigar-shaped graphite crystals with conical structure. *Carbon*, 6(3):381, 1968.
 - [13] Ivan Gutman. Irregularity of molecular graphs. *Kragujevac Journal of Science*, (38):71–81, 2016.
 - [14] Batmend Horoldagva, Lkhagva Buyantogtokh, Shiikhar Dorjsembe, and Ivan Gutman. Maximum size of maximally irregular graphs. *MATCH Commun. Math. Comput. Chem.*, 76:81–98, 2016.
 - [15] Sumio Iijima. Helical microtubules of graphitic carbon. *nature*, 354(6348):56–58, 1991.
 - [16] Kamel Jebreen. *Modèles graphiques pour la classification et les séries temporelles*. PhD thesis, Aix-Marseille, 2017.
 - [17] Kamel Jebreen, Muhammad Haroon Aftab, Iftikhar Ali, Mohammed Issa Sowaity, and Hassan Kanj. Topological aspects investigated from m-polynomial of γ -sheet of boron clusters. *International Journal of Chemical and Biochemical Sciences*, 24(4):469–477, 2023.
 - [18] Kamel Jebreen, Muhammad Haroon Aftab, MI Sowaity, B Sharada, AM Naji, and M Pavithra. Eccentric harmonic index for the cartesian product of graphs. *Journal of Mathematics*, 2022(1):9219613, 2022.
 - [19] Kamel Jebreen, Muhammad Haroon Aftab, MI Sowaity, B Sharada, AM Naji, and M Pavithra. Research article eccentric harmonic index for the cartesian product of graphs. 2022.
 - [20] Kamel Jebreen, Muhammad Haroon Aftab, Mohammad Issa Sowaity, Zeeshan Saleem Mufti, and Muhammad Hussain. An approximation for the entropy measuring in the general structure of sgsp3. *Computers, Materials and Continua*, 73:4455–4463, 2022.
 - [21] Kamel Jebreen and Badih Ghattas. Bayesian network classification: Application to epilepsy type prediction using pet scan data. In *2016 15th IEEE International Conference on Machine Learning and Applications (ICMLA)*, pages 965–970. IEEE, 2016.
 - [22] Kamel Jebreen, Hifza Iqbal, Muhammad Haroon Aftab, Iram Yaqoob, Mohammed Issa Sowaity, and Amjad Barham. Study of eccentricity based topological indices for benzenoid structure. *South African Journal of Chemical Engineering*, 45:221–227, 2023.
 - [23] Kamel Jebreen, Mohamad Motasem Nawaf, Amjad Barham, and Badih Ghattas. Inferring linear and nonlinear interaction networks using neighborhood support vector machines. In *2021 International Conference on Engineering and Emerging Technologies (ICEET)*, pages 1–6. IEEE, 2021.
 - [24] Kamel Jebreen, Marianela Petruzzelli, and Olivier C Martin. Probabilities of multi-locus genotypes in sib recombinant inbred lines. *Frontiers in genetics*, 10:833, 2019.

- [25] Kamel Jebreen, Eqbal Radwan, Wafa Kammoun-Rebai, Etimad Alattar, Afnan Radwan, Walaa Safi, Walaa Radwan, and Mohammed Alajezi. Perceptions of undergraduate medical students on artificial intelligence in medicine: mixed-methods survey study from palestine. *BMC Medical Education*, 24(1):507, 2024.
- [26] Hassan Kanj, Hifza Iqbal, Muhammad Haroon Aftab, Hasnain Raza, Kamel Jebreen, and Mohammed Issa Sowaity. Topological characterization of hexagonal network and non-kekulean benzenoid hydrocarbon. *European Journal of Pure and Applied Mathematics*, 16(4):2187–2197, 2023.
- [27] Tarek Khalifa, Nawaf Ali, Muhammad Rafaqat, Muhammad Haroon Aftab, Hassan Kanj, Mouhammad Alakkoumi, and Kamel Jebreen. Topological characterization for triangular, regular triangular oxides and silicates networks. *European Journal of Pure and Applied Mathematics*, 17(3):2106–2126, 2024.
- [28] Mark T Lusk and Lincoln D Carr. Nanoengineering defect structures on graphene. *Physical review letters*, 100(17):175503, 2008.
- [29] Inad Nawajah, Hassan Kanj, Yehia Kotb, Julian Hoxha, Mouhammad Alakkoumi, and Kamel Jebreen. Bayesian regression analysis using median rank set sampling. *European Journal of Pure and Applied Mathematics*, 17(1):180–200, 2024.
- [30] Inad Nawajah, Eqbal Radwan, Mohammed Abuharb, Hussein Jabareen, Mohannad Jazzar, Wafa Kammoun Rebai, and Kamel Jebreen. Principal component analysis of the environmental attitudes of students at faculty of economics during the covid-19 pandemic: A cross-sectional study from palestine. *Multidisciplinary Science Journal*, 7(1):2025033–2025033, 2025.
- [31] Tamas Réti, Reza Sharafdini, Agota Dregelyi-Kiss, and Hossein Haghbin. Graph irregularity indices used as molecular descriptors in qspr studies. *MATCH Commun. Math. Comput. Chem*, 79(2):509–524, 2018.
- [32] Tamas Réti, Reza Sharafdini, Agota Dregelyi-Kiss, and Hossein Haghbin. Graph irregularity indices used as molecular descriptors in qspr studies. *MATCH Commun. Math. Comput. Chem*, 79(2):509–524, 2018.
- [33] Damir Vukičević and Ante Graovac. Valence connectivity versus randić, zagreb and modified zagreb index: A linear algorithm to check discriminative properties of indices in acyclic molecular graphs. *Croatica chemica acta*, 77(3):501–508, 2004.